JCI The Journal of Clinical Investigation

# Increased islet apoptosis in *Pdx1*$^{+/-}$ mice

James D. Johnson, … , Helena Edlund, Kenneth S. Polonsky

*J Clin Invest.* 2003;111(8):1147-1160. https://doi.org/10.1172/JCI16537.

**Article** **Metabolism**

Mice with 50% *Pdx1*, a homeobox gene critical for pancreatic development, had worsening glucose tolerance with age and reduced insulin release in response to glucose, KCl, and arginine from the perfused pancreas. Surprisingly, insulin secretion in perifusion or static incubation experiments in response to glucose and other secretagogues was similar in islets isolated from *Pdx1*$^{+/-}$ mice compared with *Pdx1*$^{+/+}$ littermate controls. Glucose sensing and islet $Ca^{2+}$ responses were also normal. Depolarization-evoked exocytosis and $Ca^{2+}$ currents in single *Pdx1*$^{+/-}$ cells were not different from controls, arguing against a ubiquitous β cell stimulus-secretion coupling defect. However, isolated *Pdx1*$^{+/-}$ islets and dispersed β cells were significantly more susceptible to apoptosis at basal glucose concentrations than *Pdx1*$^{+/+}$ islets. $Bcl_{XL}$ and Bcl-2 expression were reduced in *Pdx1*$^{+/-}$ islets. In vivo, increased apoptosis was associated with abnormal islet architecture, positive TUNEL, active caspase-3, and lymphocyte infiltration. Although similar in young mice, both β cell mass and islet number failed to increase with age and were approximately 50% less than controls by one year. These results suggest that an increase in apoptosis, with abnormal regulation of islet number and β cell mass, represents a key mechanism whereby partial PDX1 deficiency leads to an organ-level defect in insulin secretion and diabetes.



# Increased islet apoptosis in *Pdx1*$^{+/-}$ mice

James D. Johnson,[1] Noreen T. Ahmed,[2] Dan S. Luciani,[3] Zhiqiang Han,[3] Hung Tran,[3] Jun Fujita,[3] Stanley Misler,[1] Helena Edlund,[4] and Kenneth S. Polonsky[3]

[1]Renal Division, Department of Internal Medicine, Washington University School of Medicine/Barnes-Jewish Hospital, St. Louis, Missouri, USA
[2]University of Chicago Pritzker School of Medicine, Chicago, Illinois, USA
[3]Metabolism Division, Department of Internal Medicine, Washington University School of Medicine/Barnes-Jewish Hospital, St. Louis, Missouri, USA
[4]Umea Center for Molecular Medicine, Umea University, Umea, Sweden

**Mice with 50% *Pdx1*, a homeobox gene critical for pancreatic development, had worsening glucose tolerance with age and reduced insulin release in response to glucose, KCl, and arginine from the perfused pancreas. Surprisingly, insulin secretion in perifusion or static incubation experiments in response to glucose and other secretagogues was similar in islets isolated from *Pdx1*$^{+/-}$ mice compared with *Pdx1*$^{+/+}$ littermate controls. Glucose sensing and islet $Ca^{2+}$ responses were also normal. Depolarization-evoked exocytosis and $Ca^{2+}$ currents in single *Pdx1*$^{+/-}$ cells were not different from controls, arguing against a ubiquitous β cell stimulus-secretion coupling defect. However, isolated *Pdx1*$^{+/-}$ islets and dispersed β cells were significantly more susceptible to apoptosis at basal glucose concentrations than *Pdx1*$^{+/+}$ islets. $Bcl_{XL}$ and Bcl-2 expression were reduced in *Pdx1*$^{+/-}$ islets. In vivo, increased apoptosis was associated with abnormal islet architecture, positive TUNEL, active caspase-3, and lymphocyte infiltration. Although similar in young mice, both β cell mass and islet number failed to increase with age and were approximately 50% less than controls by one year. These results suggest that an increase in apoptosis, with abnormal regulation of islet number and β cell mass, represents a key mechanism whereby partial PDX1 deficiency leads to an organ-level defect in insulin secretion and diabetes.**

*J. Clin. Invest.* **111**:1147–1160 (2003). doi:10.1172/JCI200316537.

## Introduction

Homeobox genes regulate organ development and morphology by controlling the fate of specific cell populations (1–4). Pancreatic duodenal homeobox-1 (PDX1), known as IPF-1 in humans, is a homeobox transcription factor that is absolutely required for the development of the pancreas and other foregut structures (5). Humans and mice that do not express the *Pdx1* gene exhibit pancreatic agenesis (6, 7). Heterozygosity for inactivating mutations of the *IPF1* gene in humans leads to MODY4, a rare form of maturity-onset diabetes of the young (MODY), in which early onset diabetes is characterized by impaired insulin secretion in response to glucose. (8). Similarly, mice with genetically engineered reductions in PDX1 levels have impaired glucose tolerance, and mice in which PDX1 has been genetically inactivated in more than 80% of the β cells develop diabetes (9–13). Based mainly on in vivo studies of these transgenic mice and experiments conducted on various cell lines, this homeobox gene has been ascribed several important "day-to-day" physiological roles in adult β cells, including glucose sensing, insulin biosynthesis, and insulin exocytosis (11). Located preferentially but not exclusively in β cells, PDX1 has been reported to influence the expression of a number of β cell genes, including those coding for insulin (14, 15), islet amyloid polypeptide (16, 17), glucokinase (13, 14, 18), and GLUT2 (11, 13, 14, 19), suggesting that PDX1 may play a broad role. Surprisingly, corresponding studies on isolated islets or β cells that might reveal a cell-autonomous, inherent defect in the ability of individual β cells to sense glucose and secrete insulin have not been reported.

Our results demonstrate that, while individual isolated *Pdx1*$^{+/-}$ islets and dispersed β cells have normal glucose signaling and stimulus-secretion coupling, *Pdx1* haploinsufficient islets exhibit significant apoptosis at basal glucose concentrations. The developmental role of PDX1 persists into adulthood through the lifelong maintenance of islet mass, architecture, and plasticity, processes that involve the interaction of β cell neogenesis, differentiation, and apoptosis (20). Although the effects are dramatically distinct compared with total PDX1 ablation, the phenotype of *Pdx1* heterozygous mice makes them a highly relevant model for study of the pathophysiology of MODY.

*Received for publication July 30, 2002, and accepted in revised form February 11, 2003.*

**Address correspondence to:** K.S. Polonsky, Department of Medicine, Washington University School of Medicine, Campus Box 8066, 660 S. Euclid Avenue, St. Louis, Missouri 63110, USA. Phone: (314) 362-8061; Fax: (314) 362-8015; E-mail: Polonsky@im.wustl.edu.

**Conflict of interest:** The authors have declared that no conflict of interest exists.

**Nonstandard abbreviations used:** pancreatic duodenal homeobox 1 (PDX1); maturity-onset diabetes of the young (MODY); intraperitoneal glucose tolerance test (IPGTT); Krebs-Ringer buffer (KRB); intracellular-like solution (IS); tetraethylammonium (TEA); pico Farad (pF).

## Methods

*In vivo characterization of mice*. *Pdx1* haploinsufficient mice used in the present study, in which exon 2 was replaced with the neomycin-resistance gene, have been described previously (6). Mice were genotyped by PCR. Unless otherwise indicated, mice were used for most experiments between 8 and 12 weeks of age to avoid potentially confounding effects of lowered total pancreatic insulin on our results (see Results below). Intraperitoneal glucose tolerance tests (IPGTTs) were performed after a 4-hour fast (2 g dextrose/kg body weight).

*Pancreatic perfusion*. Pancreata were perfused in a humidified, temperature-controlled chamber, via the aorta at the level of the celiac artery, as described elsewhere (21). Oxygenated Krebs-Ringer buffer (KRB) containing 119 mM NaCl, 4.7 mM KCl, 25 mM $NaHCO_3$, 2.5 mM $CaCl_2$, 1.2 mM $MgSO_4$, 1.2 mM $KH_2PO_4$, and 0.25% radioimmunoassay-grade BSA with the indicated concentrations of glucose was delivered at 1 ml/min using a Minipuls 3 peristaltic pump (Gilson Inc., Middleton, Wisconsin, USA). Prior to sample collection, pancreata were perfused with 5 mM glucose/KRB for 30–40 minutes. Samples were collected at 5-minute intervals. Glucose ramps were generated as previously described (21).

*Islet isolation and characterization*. Insulin content was measured by radioimmunoassay (see below) after acid/ethanol extraction from homogenized whole pancreata that had been dissected, removed from the animal, and weighed. To obtain pancreatic islets, pancreata were removed and islets were isolated by collagenase digestion using a protocol adapted (21) from one described by Lacy and Kostianovsky (22). Isolations from *Pdx1* heterozygotes older than 16 weeks usually did not yield islets. After isolation, islets were cultured for 4 hours in 10 mM glucose RPMI media (containing 100 IU/ml penicillin, 100 μg/ml streptomycin, and 10% FCS; pH was adjusted to 7.4 with NaOH) before being hand-picked and cultured overnight at 37°C with 5% $CO_2$ and saturated humidity.

*Hormone release*. For static incubations, groups of 5–10 islets were cultured (as above) in small tubes. Experiments were conducted on islets that had been washed under the experimental conditions (KRB equilibrated with 5% $CO_2$) for 30 minutes. In perifusion experiments, KRB was pumped at a rate of 1 ml/min around islets that were loaded into temperature- and $CO_2$-controlled 300-μl plastic chambers and padded on both sides with beads. Islets were washed under basal conditions for 1 hour prior to the experiment. Insulin and C-peptide were measured from in vivo and in vitro samples by radioimmunoassay (Linco Research Inc., St. Charles, Missouri, USA).

*Islet imaging*. Hand-picked islets were allowed to adhere to glass coverslips overnight prior to imaging for $Ca^{2+}$ levels or NADH autofluorescence, as described previously (21). Briefly, Fura-2 AM–loaded islets were perifused at a flow rate of 1 ml/min with KRB (no BSA) at 37°C on the stage of a Nikon inverted microscope (Nikon Inc., Melville, New York, USA). Changes in intracellular $Ca^{2+}$ within individual islets were reflected in the ratio of fluorescence emission acquired above 510 nM in response to excitation at 340 nm and 380 nm. This provides a relative indication of islet $Ca^{2+}$, which is independent of dye concentration in the tissue. NADH autofluorescence was imaged in unloaded islets excited at a wavelength of 365 nM and recorded at a wavelength of 495 nM (23).

*Cell dispersion*. Islets were gently dispersed after three consecutive 1-minute washes with $Ca^{2+}$/$Mg^{2+}$-free MEM (Mediatech Inc., Herndon, Virginia, USA) followed by a 30-second exposure to trypsin/EDTA solution (Invitrogen Corp., Carlsbad, California, USA) diluted 1:5 in MEM. This was followed by gentle repetitive pipetting and a final wash with $Ca^{2+}$/$Mg^{2+}$-free MEM. The incorporation of MEM and diluted trypsin solutions in the present protocol are modifications designed to reduce cellular stress during the dispersion process. Unless otherwise indicated, cells were cultured on glass coverslips in RPMI media (as above) and maintained at 37°C, 5% $CO_2$, and saturated humidity for 1–3 days after dispersion.

*Single-cell imaging*. Islet cell cultures were incubated with 1 μM Fura-4F AM (Molecular Probes Inc., Eugene, Oregon, USA) in RPMI for 30 minutes and rinsed in Ringer's solution (see below) for 30 minutes. Coverslips in a narrow 35°C chamber (~300 μl) were continuously perifused with preheated solutions. Cells (3–10 per image field) were excited at 340 nM and 380 nM using a monochromator (T.I.L.L. Photonics GmbH, Grafelfing, Germany) through a 20× objective (IX70; Olympus Optical Co., Tokyo, Japan, USA) and imaged with a CCD camera (T.I.L.L. Photonics GmbH). The formula of Grynkiewicz et al. (24) was used to convert 340/380 ratios to $Ca^{2+}$ determinations; these were calibrated "in vivo" by exposing cells to 10 μM ionomycin for more than 30 minutes to obtain maximum ratio, and then to 20 μM EGTA and 10 μM ionomycin to obtain minimum ratio.

$Ca^{2+}$ signal quantification was performed essentially as described (25) using waveform statistics determined automatically with a macro written for IgorPro software (WaveMetrics Inc., Lake Oswego, Oregon, USA). $Ca^{2+}$ levels during the 5 minutes prior to treatment were averaged to give a pretreatment mean for each cell. The maximum $Ca^{2+}$ determination during the treatment period was subtracted from the pretreatment average to give the maximal amplitude of the $Ca^{2+}$ signal. The time from initiation of treatment to maximal amplitude was measured, and the maximal amplitude was divided by this value to give the effective rate of rise of the $Ca^{2+}$ signal.

*Single-cell assays of hormone release and electrophysiology*. Our methods for the perforated-patch variant of whole-cell recording using an EPC 9 amplifier (Heka Elektronik, Lambrecht, Germany) have been described previously (26). The fire-polished tips of the recording pipettes contained either (a) high $K^+$ intracellular-like

solution (IS) containing 65 mM KCl, 28.4 mM $K_2SO_4$, 11.3 mM NaCl, 1 mM $MgCl_2$, 0.5 mM EGTA, 47.2 mM sucrose, and 20 mM KHEPES titrated to pH 7.3 or (b) a $Cs^+$-substituted IS containing 65 mM CsCl, 28.4 mM $Cs_2SO_4$, 11.3 mM NaCl, 1 mM $MgCl_2$, 0.5 mM EGTA, 47.2 mM sucrose, and 20 mM CsHEPES (titrated to pH 7.3). Pipettes were backfilled with the selected IS containing nystatin (250 μg/ml). Recordings were made at more than 30–32°C in standard extracellular solution containing 5.5 mM KCl, 2 mM $CaCl_2$, 1 mM $MgCl_2$, 20 mM HEPES, 144 mM NaCl, and various glucose concentrations. Giga-seals were obtained and the membrane potential was held at –70 mV except during 200-ms depolarizing steps. Membrane capacitance was estimated using the IgorPro module according to the method of Barnett and Misler (26), where a dual-frequency sine wave voltage is imposed on the cell. For recording $Ca^{2+}$ currents, the extracellular solution was modified by mole-for-mole substitution of tetraethylammonium (TEA) (30 mM) for NaCl and the patch pipette was filled with $Cs^+$-containing IS. The largest single cells were selected for recording because immunohistochemical, cell-sorting, and electrophysiological data from rodent islets suggest these are likely to be β cells.

*Quantification of apoptosis susceptibility*. We used a PCR-based method for detecting DNA ladders according to the manufacturer's instructions (ApoAlert LM-PCR Ladder Assay Kit; Clontech Laboratories Inc., Palo Alto, California, USA). Briefly, groups of five islets from *Pdx1*$^{+/–}$ and *Pdx1*$^{+/+}$ mice (three mice each, total of six mice per experiment) were cultured separately in RPMI containing various concentrations of glucose or thapsigargin, a known inducer of $Ca^{2+}$ stress–mediated apoptosis in β cells (23, 27). After 72 hours, genomic DNA was isolated with the DNeasy kit from QIAGEN Inc. (Valencia, California, USA) according to the manufacturer's instructions for cultured cells, except that islets were maintained in lysis buffer for 10 minutes at 50°C. Genomic DNA was then concentrated by ethanol precipitation and vacuum-dried before being resuspended and quantified using UV spectrophotometry. Next, 100 μg of DNA was ligated to adapters as described in the ApoAlert Kit. Short cycles of PCR that selectively amplify adapter-ligated DNA fragments over longer DNA were used. The resulting PCR products were run on 1.2% agarose/ethidium bromide gels in 0.5× tris-borate-EDTA. Gels were imaged and background-subtracted DNA ladders were quantified using densitometry (Eagle Eye II; Stratagene, La Jolla, California, USA). In order to compare data from separate gels, band intensity was normalized to the average laddering of the three groups of control islets in 5 mM glucose. Apoptosis was also measured in single dispersed cells cultured overnight as for imaging experiments using the ApoPercentage Kit (Biocolor Ltd., Newtownabbey, Northern Ireland, United Kingdom). This kit uses a dye that stains cells as they undergo the membrane "flip-flop" event when phosphatidylserine is translocated to the outer leaflet (28). This event is considered diagnostic of apoptosis but not necrosis. Apoptotic cells, which appeared bright pink against the white background of phenol red–free RPMI (Tissue Culture Support Center, Washington University, St. Louis, Missouri, USA), were counted manually in a blinded fashion.

*Analysis of gene expression by RT-PCR*. The expression of islet-specific and apoptosis-related genes was analyzed by RT-PCR according to the method described by Wong et al. (29). Fifteen islets were cultured under conditions identical to those described above for the DNA ladder assay (see *Quantification of apoptosis susceptibility*). Total RNA was isolated using the RNeasy Mini Kit (QIAGEN Inc.) with DNase I treatment and dried. RNA was reverse transcribed using SuperScript II RNase-H Reverse Transcriptase (Invitrogen Corp., Carlsbad, California, USA) with oligo $d(T)_{14–18}$ primer (Invitrogen Corp.) in 20 μl reaction volume, from which 2 μl was used for detection of insulin-1, insulin-2, glucagon, PDX1, and apoptosis-related gene transcripts using PCR. GAPDH was used as the internal standard to which mRNA levels were normalized. GAPDH expression, which did not vary under any of the conditions used, was further validated by comparing its expression to that of β-actin mRNA using QuantumRNA Universal 18S Internal Standards (Ambion Inc., Austin, Texas, USA). As a control, we ascertained that PCR of the isolated RNA samples without reverse transcriptase did not generate detectable products under these conditions (not shown). Where possible, we designed primers that overlapped intronic regions that would reveal the presence of any contaminating genomic DNA. Primer pairs and conditions used were: insulin-1 (261 bp), 5′-TCAGAGACCATCAGCAAGCAG-3′ and 5′-GTCTGAAGGTCCCCGGGGCT-3′, 19 cycles; insulin-2 (267 bp), 5′-TCAGAGACCATCAGCAAGCAG-3′ and 5′-GTCTGAAGGTCACCTGCTCC-3′, 18 cycles; glucagon (215 bp), 5′-CATTCACAGGGCACATTGACC-3′ and 5′-ACCAGCCAAGCAATGAATTCCTT-3′, 24 cycles; Pdx1 (290 bp), 5′-CCCTTTCCCGTGGATGAAATC-3′ and 5′-GGGTCCCGCTACTACGTTTCTTATC-3′, 32 cycles; GAPDH (532 bp), 5′-GGAGCCAAACGGGTCATCATCTC-3′ and 5′-AGTGGGAGTTGCTGTTGAAGTCGC-3′, 23 cycles. PCR reactions for these genes are performed at an annealing temperature of 58°C. The CytoXpress quantitative PCR Detection Kit for Mouse Apoptosis Set 2 (BioSource International, Camarillo, California, USA) was used for multiplex PCR of apoptosis-related genes (caspase-3, Bax, Bcl-2, and $Bcl_{XL}$; 32 PCR cycles). Twenty microliters of each 50-μl PCR reaction was electrophoretically separated on 2% agarose gels containing 0.5 μg/ml of ethidium bromide in tris-borate-EDTA buffer. Band intensity was analyzed by densitometry.

*Morphometry and immunohistochemistry*. Primary antibodies to rat insulin (Linco Research Inc., St. Charles, Missouri, USA), glucagon, active (cleaved) caspase-3

(Trevigen Inc., Gaithersburg, Maryland, USA), and polyclonal Ki67 (Novocastra Laboratories Ltd., Newcastle upon Tyne, United Kingdom) were used. The DeadEnd colorimetric kit for TUNEL (Promega Corp., Madison, Wisconsin, USA) was used per the manufacturer's instructions. MIN6 cells exposed to 1 μM thapsigargin were used as positive controls for active caspase-3 and TUNEL staining. For measurements of islet cell area, islet architecture, and in vivo apoptosis, paraffin-embedded pancreatic tissue sections were stained red with primary antibody/3-amino,9-ethyl-carbazole and counterstained with hematoxylin (Zymed Laboratories Inc., South San Francisco, California, USA). Slides were viewed through the 1.25× or 20× objective of an Olympus BX41 microscope (Olympus Optical Co., Tokyo, Japan). Images were recorded on a Nikon Coolpix 995 digital camera. Where necessary, multiple images were spliced using Adobe Photoshop (Adobe Systems Inc., Mountain View, California, USA). Shading defects and non-red background irregularities from spliced, monochromatized images were canceled by subtracting the red channel from the green channel using MetaMorph software (Universal Imaging Corp., Downingtown, Pennsylvania, USA). Pancreatic area and β cell area were each estimated using the intensity thresholding function of the integrated morphometry package in MetaMorph. Investigators were blinded to the source of the tissue throughout the morphometric analysis. Unless otherwise specified, images are representative of one to four sections from a total of 11 *Pdx1*$^{+/+}$ and ten *Pdx1*$^{+/-}$ mice shown to have a specific phenotype by IPGTT or fasting glucose levels.

*Statistical analysis*. Results are expressed as mean ± SEM. Differences between means were evaluated using ANOVA or the Student *t* test as appropriate. Differences were considered significant at $P < 0.05$.

## Results

*Glucose tolerance tests and insulin secretion from the perfused pancreas*. *Pdx1*$^{+/-}$ mice showed elevated blood glucose concentrations compared with *Pdx1*$^{+/+}$ littermate controls (Figure 1a), as has been reported previously (11). While blood glucose levels were markedly higher at all timepoints in male *Pdx1*$^{+/-}$ mice, the effect of the mutation was less impressive in females. Subsequent experiments were conducted on male mice.

Insulin secretory function of the whole pancreas was studied using the in situ perfused pancreas. *Pdx1*$^{+/-}$ pancreata showed attenuated first-phase insulin secretion (significant at the first two timepoints) in response to a stepwise increase in glucose concentration from 5 mM to 20 mM glucose. Similarly, insulin release in response to 20 mM KCl was reduced in *Pdx1*$^{+/-}$ pancreata compared with controls (Figure 1b). The differences in glucose-stimulated insulin secretion from the whole pancreas were most apparent when glucose was increased linearly from 2 mM to 26 mM over 90 minutes and were significant above 10 mM glucose (72% reduction overall). In the continued presence of 26 mM glucose, the large response to 20 mM arginine was also reduced in *Pdx1*$^{+/-}$ pancreata (Figure 1c). Taken together, these results indicate that reduced PDX1 levels impair the appropriate response to glucose and other secretagogues. However, the function of individual islets and β cells cannot be determined from glucose tolerance tests and perfused pancreas experiments. Additional functional and morphological studies were therefore performed on isolated islets and dispersed β cells.

*Functional characterization of isolated islets*. We consistently found that the islet isolation procedure produced very few islets (always fewer than 100, decreasing with age) from *Pdx1*$^{+/-}$ mice compared with *Pdx1*$^{+/+}$ mice (almost always >200 islets). Isolated *Pdx1*$^{+/-}$ islets appeared fragmented and were slightly smaller, as noted by others (9). Experiments were done on isolated islets

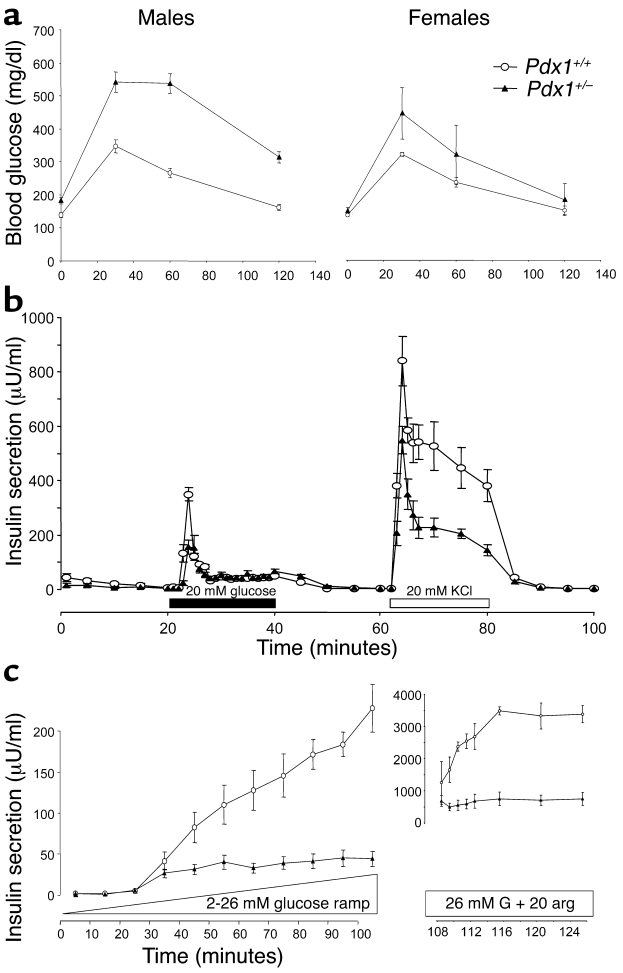


**Figure 1**
Glucose tolerance and secretagogue-induced pancreatic insulin release in *Pdx1*$^{+/-}$ mice. (**a**) IPGTTs are shown for males ($n = 9$ *Pdx1*$^{+/+}$; $n = 8$ *Pdx1*$^{+/-}$) and females ($n = 3$ *Pdx1*$^{+/+}$; $n = 3$ *Pdx1*$^{+/-}$). (**b**) Insulin release from perfused pancreata of male *Pdx1*$^{+/+}$ ($n = 5$) and *Pdx1*$^{+/-}$ ($n = 5$) mice in response to stepwise increases to 20 mM glucose (black bar) and 20 mM KCl (white bar). (**c**) Insulin release from perfused pancreata of *Pdx1*$^{+/+}$ ($n = 3$) and *Pdx1*$^{+/-}$ ($n = 3$) mice in response to a linear elevation from 2 mM to 26 mM glucose. Insulin secretion in response to 20 mM arginine (arg) was assayed in the continued presence of 26 mM glucose (G) (note the different scale). Data are from mice 8–10 weeks of age.

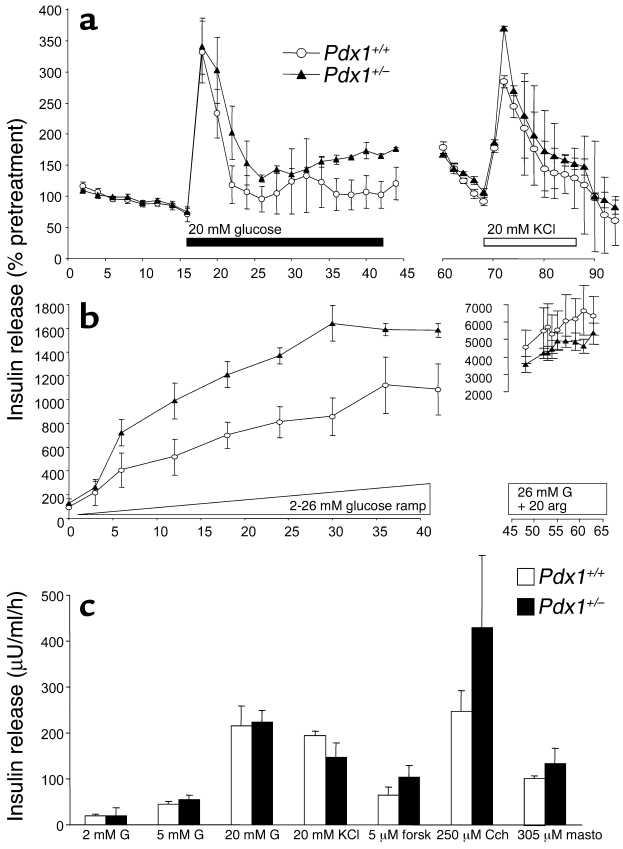


**Figure 2**
Evoked insulin release from populations of size-matched isolated islets is not altered in *Pdx1*$^{+/-}$ mice. (**a**) Perifused islets were exposed to 20 mM glucose (black bar) and 20 mM KCl (white bar) in the same experiments. Islets from three mice of each genotype were compared. Thirty to fifty islets/column were used. Insulin secretion is normalized to pretreatment values to allow pooling of columns with different basal insulin release. Basal insulin release was approximately 1.5 μU/ml/h. (**b**) The response of *Pdx1*$^{+/+}$ and *Pdx1*$^{+/-}$ islets to a ramp increase to 26 mM glucose is shown ($n$ = 4). In the presence of 26 mM glucose, islets were challenged with 20 mM arginine (right). Note the different scale. (**c**) Groups of five physically similar islets from *Pdx1*$^{+/-}$ mice or littermate controls were incubated for 1 hour in 2 mM glucose (G) ($n$ = 33), 5 mM glucose ($n$ = 12), 20 mM glucose ($n$ = 33), or 2mM glucose plus either 20 mM KCl ($n$ = 23), 5 μM forskolin ($n$ = 12), 250 μM carbachol ($n$ = 6), or 30 μM mastoparan ($n$ = 15). Unless otherwise indicated, 2 mM glucose was used. forsk, forskolin; Cch, carbachol; masto, mastoparan.

from *Pdx1*$^{+/-}$ mice that were shown to have abnormal glucose tolerance compared with control *Pdx1*$^{+/+}$ mice. Islets of similar size and apparent structural integrity were hand-picked to ensure fair comparison. Although a reduction of approximately 50% in PDX1 in this population of islets is confirmed by RT-PCR (see Figure 6b), Figure 2a shows that there were no differences in acute insulin release in response to a stepwise increase to 20 mM glucose between *Pdx1*$^{+/-}$ islets and *Pdx1*$^{+/+}$ islets. Similarly, insulin secretion induced by 20 mM KCl was not reduced in *Pdx1*$^{+/-}$ islets. Insulin secretion was also not decreased in the *Pdx1*$^{+/-}$ islets during a glucose ramp (Figure 2b). The response to 20 mM arginine, applied after the glucose ramp, was not different between the two groups of islets. We used 1-hour static incubations to compare the insulin secretory responses of *Pdx1*$^{+/-}$ and *Pdx1*$^{+/+}$ islets of similar size to glucose, KCl, and other modulators of β cell secretion. Insulin secretion was similar from the two groups of islets exposed to 2 mM, 5 mM, or 20 mM glucose (Figure 2c). At basal glucose, insulin release from islets was also similar when voltage-gated $Ca^{2+}$ channels were directly activated with 30 mM KCl and when adenylyl cyclase was activated with 5 μM forskolin. Insulin release was similar in response to 250 μM carbachol, which mobilizes inositol trisphosphate–sensitive intracellular $Ca^{2+}$ stores. Mastoparan (30 μM), which is thought to directly stimulate β cell exocytosis distal to glucose signaling, evoked similar insulin release in *Pdx1*$^{+/-}$ and *Pdx1*$^{+/+}$ islets. Collectively, the results from perifusion and static incubation of size-matched intact islets suggest that insulin secretory physiology is normal in isolated *Pdx1*$^{+/-}$ islets.

To further examine the possible effects of PDX1 deficiency on various signaling pathways, we recorded changes in intracellular $Ca^{2+}$ and NADH autofluorescence from physically similar islets. The total $Ca^{2+}$ response, reflected in the average ratio values above basal autofluorescence (area under curve divided by time ), was not significantly different with activation of metabolic pathways using 20 mM glucose, 10 mM glyceraldehyde, or 10 mM α-ketoisocaproic acid (Figure 3a). PDX1 expression did not alter the responses to 30 mM KCl or 250 μM carbachol, suggesting that $Ca^{2+}$ signaling through voltage-gated $Ca^{2+}$ channels and intracellular $Ca^{2+}$ stores was normal. In agreement with the above insulin secretion and $Ca^{2+}$ imaging results, both groups of islets generated similar changes in NADH autofluorescence during exposure to 14 mM glucose compared with controls, further suggesting that glucose signaling remains unaffected in large, intact *Pdx1*$^{+/-}$ islets (Figure 3b).

*$Ca^{2+}$ signaling and exocytosis in single cells.* To obtain a direct, quantitative assessment of β cell $Ca^{2+}$ homeostasis and responsiveness, we imaged cytosolic $Ca^{2+}$ in single cells dispersed from *Pdx1*$^{+/-}$ and control islets. However, it should be noted that because the islet dispersion requires the maximum amount of starting material, all islets isolated from a given mouse, regardless of their physical condition, were used. Many dispersed *Pdx1*$^{+/-}$ cells failed to adhere to the coverslips and displayed signs of cell death (e.g., blebbing), resulting in fewer cells per coverslip.

Resting cytosolic $Ca^{2+}$ was not significantly different between adherent *Pdx1*$^{+/-}$ (145 ± 16) and control *Pdx1*$^{+/+}$ (161 ± 16 nM) islet cells. The response to 15 mM glucose was comparable between cells from *Pdx1*$^{+/-}$ islets (63%) and control islets (68%; Figure 3, c and e). Normal mouse islets contain 60–80% β cells. The majority of glucose-stimulated $Ca^{2+}$ signals in both cell

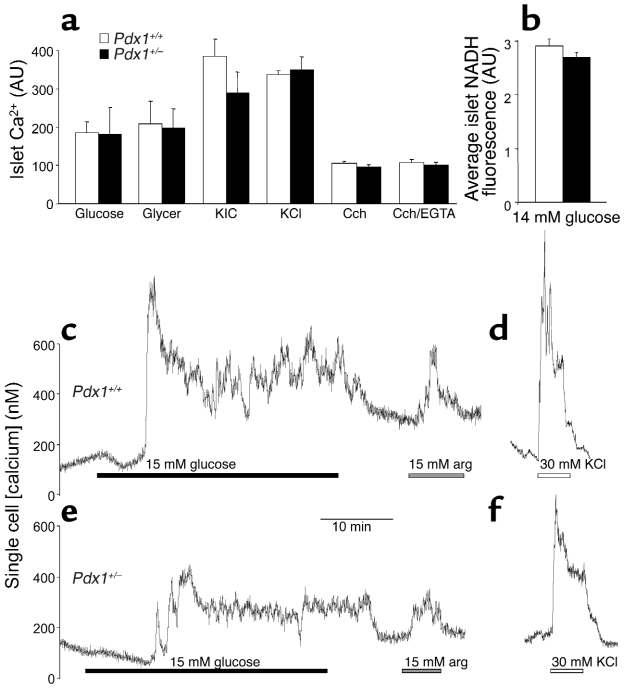


**Figure 3**
Estimation of intracellular $Ca^{2+}$ signals in islets and single β cells. (**a**) No differences were seen in $Ca^{2+}$ signals from whole islets loaded with Fura-2 in response to 20 mM glucose ($n$ = 20), 10 mM glyceraldehyde (Glycer; $n$ = 12), 10 mM α-ketoisocaproic acid (KIC; $n$ = 12), 20 mM KCl ($n$ = 50), or carbachol (Cch; in the presence or absence of 2 mM EGTA; $n$ = 8 for each). Average area under the curve (arbitrary units [AU]) was calculated from raw traces consisting of unitless ratio values (340/380). (**b**) Average NADH autofluorescence (AU) was measured from groups of individual islets ($n$ = 8). Calibrated $Ca^{2+}$ traces are shown for single, large Fura-4F–loaded *Pdx1*$^{+/+}$ cells (**c** and **d**) or *Pdx1*$^{+/-}$ cells (**e** and **f**) exposed to 15 mM glucose (black bars), 15 mM arginine (gray bars), or 30 mM KCl (white bars). Representative traces from 66 *Pdx1*$^{+/+}$ cells and 35 *Pdx1*$^{+/-}$ cells are shown. Similar results were seen with 20 mM glucose (not shown). See Table 1 for a full quantification of single-cell $Ca^{2+}$ signals. arg, arginine.

types was found in the larger cells. $Ca^{2+}$ signals were evoked by 15 mM arginine in 75% of *Pdx1*$^{+/-}$ cells versus 68% of *Pdx1*$^{+/+}$ cells. Depolarization with 30 mM KCl generated $Ca^{2+}$ signals in 97% of *Pdx1*$^{+/-}$ cells and 99% of control cells (Figure 3, d and f). Next, the $Ca^{2+}$ signals in response to 15 mM glucose, 15 mM arginine, and 30 mM KCl were analyzed statistically (Table 1). In general, $Ca^{2+}$ signals from *Pdx1*$^{+/-}$ cells were smaller and slower than those from *Pdx1*$^{+/+}$ controls. Together, these results suggest that, when cells from all islets are examined, there is a general trend toward reduced responses in cells with only one allele of *Pdx1*.

We examined ionic currents and exocytosis from large single β cells using patch-clamp electrophysiology and the capacitance technique. Single-cell electrophysiology requires the maintenance of a tight seal between the recording pipette and the cell membrane, thereby selecting for a population of cells that do not show features of end-stage apoptosis. Obtaining tight seals was consistently more difficult in *Pdx1*$^{+/-}$ cultures. Interestingly, on average, *Pdx1*$^{+/-}$ cells in the electrophysiology experiments were significantly smaller than the controls (basal membrane capacitance of 3.9 ± 0.5 *Pdx1*$^{+/-}$ vs. 5.2 ± 0.2 *Pdx1*$^{+/+}$ pico Farad (pF), suggesting a possible role for PDX1 in the regulation of cell size. The peak current (*Pdx1*$^{+/-}$, 37 ± 11 pA; *Pdx1*$^{+/+}$, 41 ± 5 pA) and current-voltage properties of the voltage-gated $Ca^{2+}$ currents were not different between cells from *Pdx1*$^{+/-}$ and *Pdx1*$^{+/+}$ islets (Figure 4a). This result did not depend on whether $Ca^{2+}$ currents were normalized to basal cell capacitance (*Pdx1*$^{+/-}$, 6.7 ± 1.2 pA/pF; *Pdx1*$^{+/+}$, 7.4 ± 0.6 pA/pF).

The secretory response to a train of twenty 200-ms depolarizations, as assayed by the increase in membrane capacitance, was not different between *Pdx1*$^{+/-}$ and *Pdx1*$^{+/+}$ β cells (summarized in Figure 4b), regardless of whether recordings were made in using a standard high-$K^+$ pipette (data not shown) or using a $Cs^+$ pipette and 30 mM TEA in the bath to simultaneously measure $Ca^{2+}$ currents (Figure 4, c and d). Exocytosis as a percentage of basal surface area was virtually identical in the cells tested (*Pdx1*$^{+/-}$, 7.2 ± 2.4%; *Pdx1*$^{+/+}$, 7.6 ± 1.6%). In the later set of experiments, forskolin (10 μM) was added to the bath to mimic paracrine factors and enhance secretion (30). In both cell types, exocytosis could be enhanced by agents that increase cAMP (data not shown), suggesting that pathways coupled to paracrine hormones are intact. These results strongly suggest that the components mediating $Ca^{2+}$-dependent exocytosis are not affected by a reduction of approximately 50% in PDX1 expression, at least in the population of seemingly healthy cells from which recordings can be made.

*Susceptibility to apoptosis in Pdx1*$^{+/-}$ *islets.* Our observations of isolated islets and dispersed cells described above suggested a role for PDX1 in regulation of β cell survival.

**Table 1**
Quantification of $Ca^{2+}$ signals

| | *Pdx1*$^{+/+}$ | *Pdx1*$^{+/-}$ |
|---|---|---|
| Resting $[Ca^{2+}]_i$ | 161 ± 16 nM | 145 ± 16 nM |
| Response, 15 mM glucose | 68% | 63% |
| Maximal amplitude | 485 ± 51 nM | 329 ± 35 nM[A] |
| Time to peak | 510 ± 53 s | 737 ± 52 s[A] |
| Rate of rise | 1.3 ± 0.16 nM/s | 0.52 ± 0.09 nM/s[A] |
| Response to 15 mM arginine | 68% | 75% |
| Maximal amplitude | 422 ± 51 nM | 218 ± 32 nM[A] |
| Time to peak | 78 ± 13 s | 124 ± 28 s[A] |
| Rate of rise | 9.6 ± 2.1 nM/s | 3.25 ± 1.2 nM/s[A] |
| Response, 30 mM KCl | 99% | 97% |
| Maximal amplitude | 591 ± 47 nM | 341 ± 16 nM[A] |
| Time to peak | 92 ± 17 s | 127 ± 8 s[A] |
| Rate of rise | 6.2 ± 1.1 nM/s | 5.6 ± 0.6 nM/s |

Intracellular (i) $Ca^{2+}$ signals from single Fura-4F–loaded islet cells were quantified as described in Methods. Cells were obtained from all isolated islets (i.e., not hand-picked or size-matched). Maximal amplitude is calculated as maximum increase from baseline. Rate of rise is calculated as maximal amplitude/time to maximal amplitude. [A]Significantly different from control. KCl, potassium chloride.

In order to test this hypothesis in vitro, apoptosis was measured using two independent techniques in islets and dispersed islet cells from *Pdx1*$^{+/-}$ and *Pdx1*$^{+/+}$ mice. DNA laddering is a common and specific endpoint of many apoptotic pathways and has been demonstrated previously in islets and β cells undergoing programmed cell death. A semiquantitative PCR-based method to detect DNA ladders demonstrated that *Pdx1*$^{+/-}$ islets cultured in 5 mM or 10 mM glucose for 72 hours showed a significant increase in apoptosis compared with physically similar control islets (Figure 5, a and b). It is notable that this probably reflects enhanced apoptosis under physiological conditions since differences were not significant at high glucose (25 mM) or $Ca^{2+}$ stress (10 μM thapsigargin).

To confirm the finding of increased apoptosis using an independent method and to extend it to dispersed single islet cells, an apoptosis-specific live dye was used. This dye is selectively incorporated into apoptotic cells when phosphatidylserine is translocated to the outer leaflet of the plasma membrane, a hallmark of apoptosis (28). This experiment revealed a higher proportion of *Pdx1*$^{+/-}$ cells actively undergoing apoptosis compared with *Pdx1*$^{+/+}$ cells (Figure 5c). This confirmed the previous impressions, based on cell loss and membrane blebbing, that dispersed *Pdx1*$^{+/-}$ cells were undergoing an abnormally high rate of apoptosis in culture. Together, these findings strongly suggest that *Pdx1*$^{+/-}$ islets and β cells are more susceptible to apoptosis.

Gene expression patterns were examined in *Pdx1*$^{+/-}$ and control islets cultured in various glucose concentrations and in thapsigargin. Multiplex semiquantitative RT-PCR revealed significant decreases in the expression of the antiapoptotic genes $Bcl_{XL}$ and Bcl-2 in islets cultured at 10 mM or 25 mM glucose, with no changes in Bax or caspase-1 (Figure 6a). RT-PCR of the same samples was also used to confirm downregulation of PDX1 mRNA in cultured islets and to assay the expression of insulin and glucagon genes (Figure 6, b–d). These results show that PDX1 levels are not modulated over 72 hours by elevated glucose and/or proapoptotic conditions in *Pdx1*$^{+/-}$ or control islets. Similarly, the expression of insulin at physiological glucose concentrations was not different in *Pdx1*$^{+/-}$ islets, although there was a reduction in insulin-1 mRNA at 25 mM glucose. Overall, the expression of insulin-1, insulin-2, or glucagon mRNA was not dramatically altered by the culture conditions, although a trend toward underexpression of insulin and overexpression of glucagon is suggested.

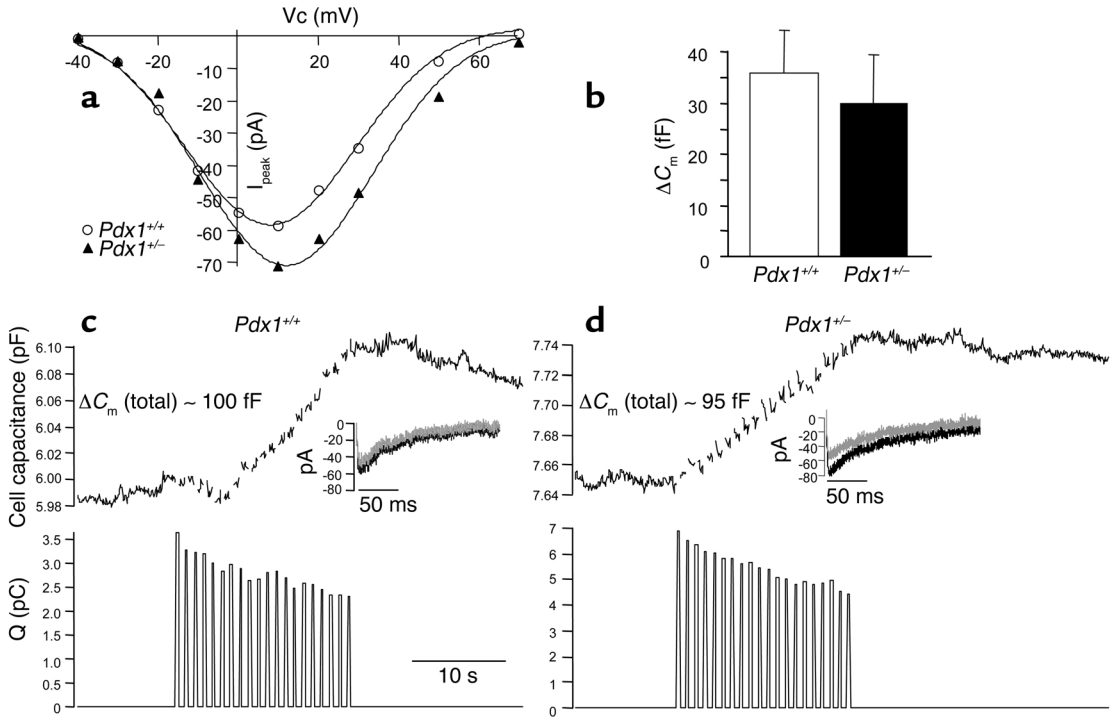


**Figure 4**

Single-cell exocytosis and voltage-gated $Ca^{2+}$ currents are not altered in β cells from PDX1 transgenic mice. (**a**) A representative *I*/*V* curve made from consecutive (same-day) recordings of two *Pdx1*$^{+/-}$ and two *Pdx1*$^{+/+}$ cells is shown. Analysis of voltage-gated Ca channels was performed on cells dispersed from six *Pdx1*$^{+/+}$ and six *Pdx1*$^{+/-}$ mice. $V_C$, voltage. (**b**) Stimulated exocytosis is intact in *Pdx1*$^{+/-}$ β cells. Results from both standard and TEA-treated conditions were pooled, and these results are summarized (*n* = 33 for *Pdx1*$^{+/+}$; *n* = 30 for *Pdx1*$^{+/-}$). $C_m$, membrane capacitance. Examples of changes in capacitance evoked by a train of 20 depolarizations (200 ms) from a holding potential of –70 mV to +10 mV in patch-clamped cells from *Pdx1*$^{+/+}$ (**c**, top panel) and *Pdx1*$^{+/-}$ (**d**, top panel) islets. Recordings were made using a $Cs^+$ pipette, with 30 mM TEA in the bath to simultaneously measure voltage-gated $Ca^{2+}$ currents. Integrated $Ca^{2+}$ charge entry is shown for each depolarization (bottom panels). $Ca^{2+}$ current traces are shown for the first and 20th depolarizations (insets). Q(pC); charge entry; fF, femto Ferad.

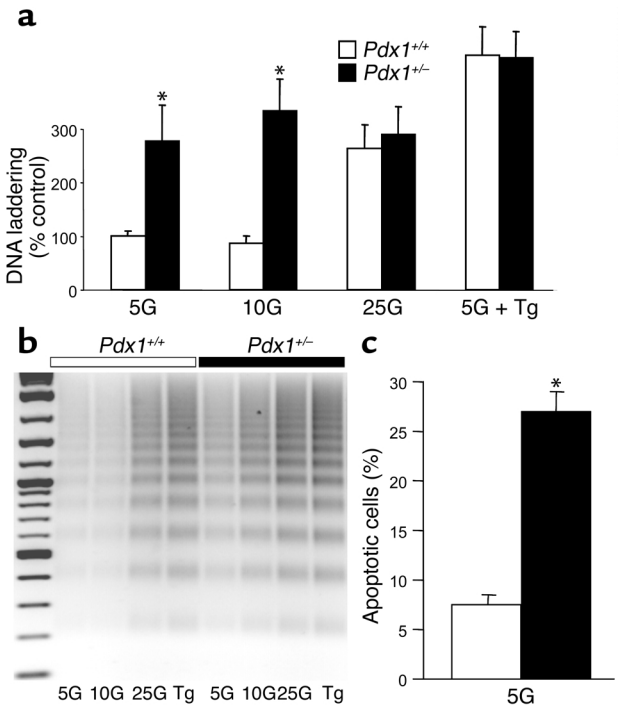


**Figure 5**

*Pdx1*$^{+/-}$ islets and cells are prone to apoptosis when cultured in low glucose concentrations. (**a**) Apoptosis, measured by PCR-enhanced DNA laddering, was compared in groups of five islets cultured in RPMI with 5 mM, 10 mM, and 25 mM glucose for 72 hours ($n$ = 10 for each genotype). Islets cultured in 10 μM thapsigargin (Tg), a known inducer of islet apoptosis, were used as a positive control. Apoptotic calf-thymus DNA served as an additional reference control, independent of our cultures. DNA-ladder bands were quantified by densitometry and pooled as described in Methods. (**b**) A representative gel is shown. (**c**) The average percentage of apoptotic cells measured in dispersed islet cells cultured overnight in 5 mM glucose, measured by cell uptake of a specific dye (Methods). Cells were counted manually in phenol red–free RPMI. Shown are pooled results from three coverslips of islets dispersed from three mice of each genotype. Asterisks denote significant differences.

In order to put these apoptosis experiments into context with the secretion experiments, the media supernatants from the DNA-ladder experiments was saved and analyzed for hormone secretion. Long-term C-peptide secretion was not significantly different in *Pdx1*$^{+/-}$ islets under any of the conditions used (data not shown). These results suggest that the apoptosis-related defect in functional islet cell mass precedes a defect in glucose-stimulated insulin secretion and may also suggest that a subpopulation of islets or islet cells is sufficient to maintain normal response to glucose over 72 hours.

*Analysis of pancreatic morphology and β cell mass.* To determine whether enhanced apoptosis and its eventual consequence, reduced β cell mass, could be detected in vivo, we examined pancreas sections from *Pdx1*$^{+/-}$ and *Pdx1*$^{+/+}$ mice at 3, 5, and 12 months of age. At all ages studied, *Pdx1*$^{+/-}$ mice showed glucagon-positive α cells within the core of a large percentage of islets (Figure 7). Glucagon staining was observed within the cores of 1-year-old islets from both genotypes. In agreement with a previous report (9), we observed an increased ratio of α cells to β cells in younger *Pdx1*$^{+/-}$ islets. At higher magnification, adjacent sections showed some islets with cells staining positive for both insulin and glucagon, as previously described for the β cell–specific PDX1 knockout (11). Immunohistochemistry for the proapoptotic (cleaved) form of caspase-3 revealed sporadic staining that was more common in *Pdx1*$^{+/-}$ islets and increased substantially with age (Figure 8, a–d). Similarly, TUNEL-positive cells, though rare, were found almost exclusively in islets (Figure 8, e–h) and acinar cells (not shown) of *Pdx1*$^{+/-}$ mice. Frequently *Pdx1*$^{+/-}$ islets showed marked expansion of the islet microvasculature compared with controls. However, even at 1 year of age, some *Pdx1*$^{+/-}$ islets showed no signs of damage or apoptosis. Together, these findings provide direct evidence for the regulation of apoptosis by PDX1 in vivo.

The low frequency of cells staining positive for TUNEL or active caspase-3 was not unexpected since apoptotic cells are rapidly cleared by the immune system in vivo. Although more common in 12-month-old animals, we observed lymphocyte infiltration at the periphery of islets in *Pdx1*$^{+/-}$ mice of all ages, suggesting an immune response. Some of the infiltrating lymphocytes exhibited TUNEL staining (Figure 9a) or cleaved caspase-3 immunoreactivity (not shown). Staining for Ki67, a nuclear antigen specific to proliferating cells, revealed clusters of positive cells in the invading lymphocytes in *Pdx1*$^{+/-}$ islets (Figure 9b), confounding attempts to quantify β cell proliferation.

Finally, we asked whether the apoptotic effects of *Pdx1* haploinsufficiency correspond to altered islet survival or neogenesis in vivo by assessing pancreatic β cell mass. Unlike wild-type mice, which compensate for age with increased β cell mass, 1-year-old *Pdx1*$^{+/-}$ mice had a greater than 50% reduction in normalized β cell surface area compared with littermate controls. This difference was due to approximately 50% fewer islets, rather than a significant decrease in the average area of individual isles. (Figure 10). The change in β cell mass was mirrored by a decrease in normalized pancreatic insulin content in older *Pdx1*$^{+/-}$ mice (expressed as ng/ml/mg pancreatic weight: *Pdx1*$^{+/-}$, 226 ± 38; *Pdx1*$^{+/+}$, 521 ± 70), but not at 8–10 weeks (*Pdx1*$^{+/-}$, 560 ± 27 ng/ml/mg; *Pdx1*$^{+/+}$, 491 ± 42 ng/ml/mg; $n$ = 6 for each genotype and age). The reduction in pancreatic insulin content was significant whether expressed as an absolute or normalized to pancreatic weight. Animal weights and pancreatic weights were not different at any age studied. Therefore, lower pancreatic insulin content in older mice can be explained by a decreased number of functional islets, rather than a reduction in insulin stored in single β cells. The substantial decrease in β cell mass over time, along with defects in architecture and differentiation of some islets, support the idea that *Pdx1*$^{+/-}$ islets undergo apoptosis and dedifferentiation in vivo.

## Discussion

The present study was undertaken to explore the mechanisms responsible for the defective insulin secretion resulting from decreased expression of PDX1 in mice in vivo. The two major findings are as follows. First, islets and single β cells isolated from *Pdx1*$^{+/-}$ mice (expressing 50% of the normal levels of PDX1) can demonstrate normal glucose sensing, stimulus-secretion coupling, and insulin secretion. Second, a 50% reduction in PDX1 predisposes islets to apoptosis in vitro and in vivo, leading to disrupted islet architecture and eventually to a marked decrease in β cell area and islet number. Since the maintenance of adequate insulin secretion involves the relative rates of β cell proliferation/neogenesis and death, these findings identify an important factor contributing to the complex phenotype of *Pdx1*$^{+/-}$ mice. They suggest that PDX1 plays an important role in the development and maintenance of an adequate pool of healthy islets in the adult animal in addition to its well established role in

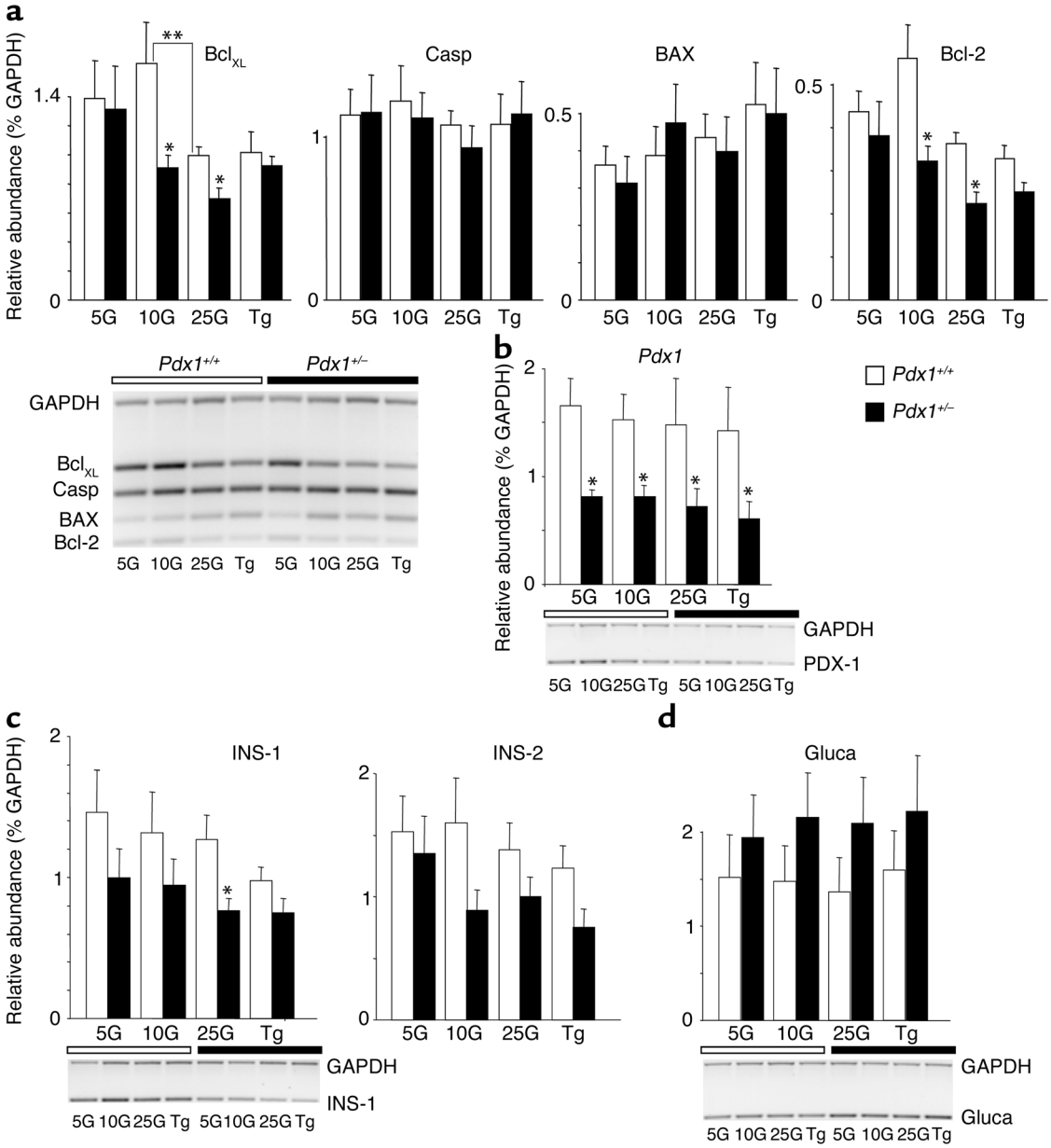


**Figure 6**

RT-PCR analysis of gene expression. (**a**) The densitometric quantification of four apoptosis-related genes — Bcl$_{XL}$, caspase-3 (Casp), BAX, and Bcl-2 — relative to GAPDH in cultured islets (cultured as in Figure 5) is quantified by densitometry (above). Data are pooled from four gels (representative example shown below). White bars over gel images denote *Pdx1*$^{+/+}$ islets, while black bars denote *Pdx1*$^{+/-}$ islets. Each RT-PCR sample was pooled from the cultured islets of three mice. (**b**–**d**) Relative abundance of PDX1, insulin-1 (Ins-1), insulin-2 (Ins-2), and glucagon (Gluca) mRNA are quantified from the same samples. Single asterisks denote significant differences between *Pdx1*$^{+/-}$ and *Pdx1*$^{+/+}$ islets. Double asterisks denote significant differences between different treatments to the same type of islet. Insulin content per islet protein was also not reduced in *Pdx1*$^{+/-}$ islets (not shown).

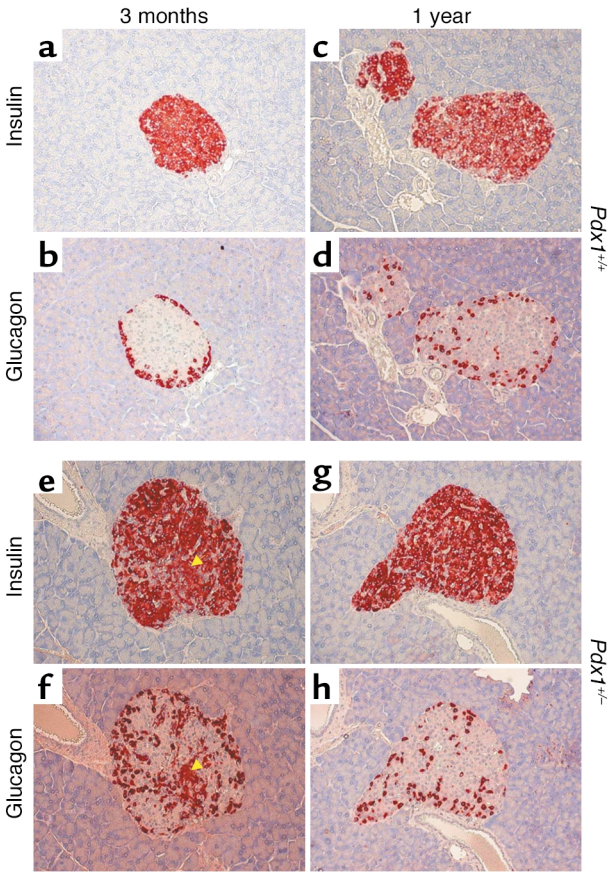


**Figure 7**
β cell and α cell architecture in *Pdx1*$^{+/-}$ islets. Insulin (**a**, **c**, **e**, and **g**) and glucagon (**b**, **d**, **f**, and **h**) are stained red in adjacent 5-μm-thick sections. *Pdx1*$^{+/-}$ islets from 3-month-old mice show striking disruption of islet architecture compared with littermate controls. Note the presence of cells stained for insulin and glucagon in **e** and **f** (arrowheads). Localization of α cells to the periphery was reduced in 1-year-old mice from both groups.

embryonic development (5, 6). The link between PDX1 and apoptosis is consistent with studies of other homeobox genes in a wide variety of model systems. Indeed, a large body of literature now suggests that the suppression of apoptosis represents a critical role of homeobox genes (2–4, 31–34).

The observation that PDX1 plays a role in the regulation of apoptosis is consistent with evidence from other experimental systems. The sand rat, *Psammomys obesus*, has extremely low PDX1 expression and develops type 2 diabetes associated with increased islet apoptosis in vivo and in vitro under specific experimental conditions (35–37). PDX1 expression is also downregulated in overtly diabetic ZDF rats (38), but can be restored by normalization of hyperglycemia (39). Glucagon-like peptide-1, which has been found to stimulate islet growth and development, increases PDX1 expression (40). Several studies have shown that PDX1 expression/activity is decreased coincidentally with β cell apoptosis or conditions known to induce β cell death, especially hyperglycemia (38, 41–46). For example, PDX1 expression is reduced during human islet apoptosis in response to high glucose (41). Under the 72-hour culture conditions used in our study, PDX1 levels did not vary significantly, suggesting that high glucose or apoptosis per se are not universal regulators of PDX1 levels.

The present findings suggest that changes in islet survival may require chronic alterations in PDX1 and can also account for the age-dependent decline in glucose tolerance seen in this and other studies (12, 13). The requirement for long-term PDX1 deficiency in the development of an in vivo phenotype was especially striking in two studies of inducible PDX1 knockouts. In one study, at least 3 weeks of doxycycline exposure was required to induced glucose intolerance, although

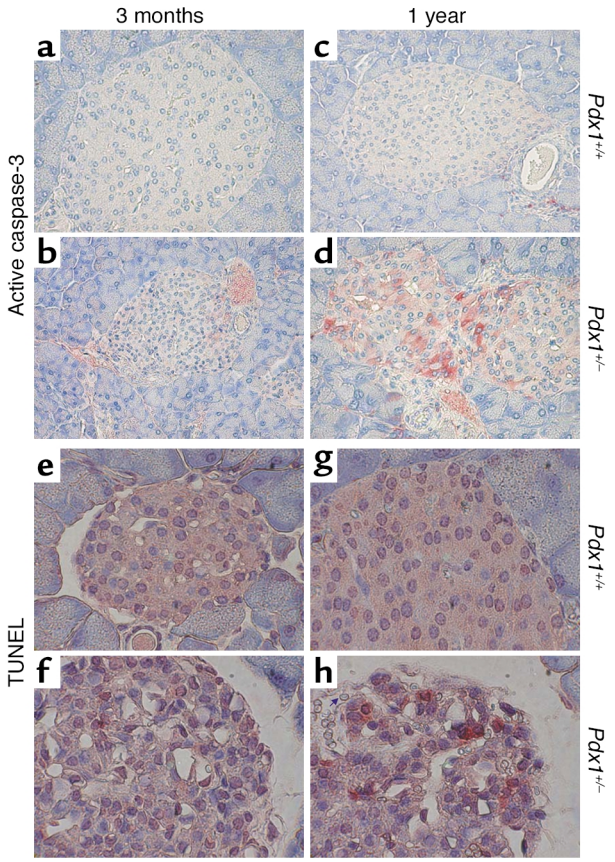


**Figure 8**
Immunohistochemistry for proapoptotic active caspase-3 and TUNEL. (**a**–**d**) *Pdx1*$^{+/-}$ islets showed modest activation of caspase-3 in vivo (red staining) compared with *Pdx1*$^{+/+}$ islets. The difference was most prominent in older animals and varied between islets from the same pancreas section. (**e**–**h**) TUNEL-positive cells (red) are seen in *Pdx1*$^{+/-}$ islets at all ages studied but are extremely rare in *Pdx1*$^{+/+}$ islets. Note the loss of intact islet structure and the striking increase in vascularization in *Pdx1*$^{+/-}$ islets (arrow in **h** points to one of many red blood cells within the islet). Islet structure and TUNEL staining was also different in *Pdx1*$^{+/-}$ islets at 5 months of age (not shown).

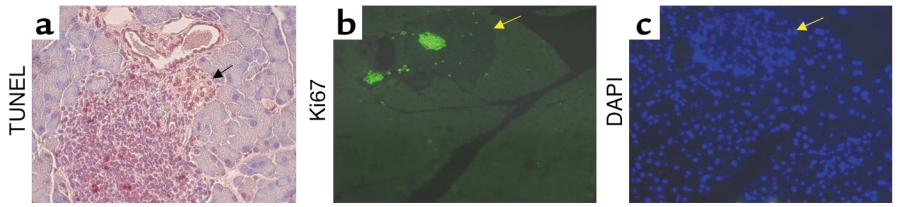


**Figure 9**
Evidence of enhanced pancreatic immune activity in *Pdx1*$^{+/-}$ mice. Infiltration of lymphocytes, some positive for TUNEL (**a**), were seen within or around islets (arrow) in old mice. Immunofluorescent localization of Ki67 nuclear antigen (**b**) reveals proliferation of lymphocytes within *Pdx1*$^{+/-}$ islets (arrows in **b** and **c** point to the same islet, also delineated by higher-density nuclear DAPI staining (**c**). Infiltrating lymphocytes are distinguished from islet cells by their small size and low-intensity nuclear staining with DAPI.

the PDX1 antisense RNA was induced within 24 hours (10). Similarly, after chronic doxycycline treatment, fasting hyperglycemia was seen in 18-month-old, but not 8-month-old, mice transgenic for an inducible PDX1 antisense/ribozyme construct capable of reducing PDX1 expression in transfected β cells within 72 hours (12). It has been noted that in humans, the severity of the PDX1 mutation correlates with age of diabetes onset (12, 47–49). Interestingly, results from inducible and classical transgenic models of PDX1 deficiency concur with our findings that males are preferentially affected (13).

The mechanism by which PDX1 affects apoptosis is unclear. However, the coinciding reduction of $Bcl_{XL}$ and Bcl-2 gene expression (and their expression relative to Bax) at 10 mM glucose points to established mediators of β cell apoptosis. It is also possible that the susceptibility to apoptosis may be related to the subtle changes in $Ca^{2+}$ signaling seen in *Pdx1*$^{+/-}$ cells. Calcium fluxes regulate many cellular functions in neuroendocrine cells, including metabolism, gene transcription, protein synthesis, protein sorting/packaging, and exocytosis (50). $Ca^{2+}$ dysregulation has been implicated in apoptosis in many cell types (51). In excitable cells such as neurons and β cells, moderately elevated $Ca^{2+}$ and electrical activity may have protective effects.

Evidence is emerging that PDX1 may act downstream of prosurvival autocrine insulin signaling in β cells. PDX1 can be activated by insulin and its downstream signaling elements, such as Foxo1 (52, 53). Recently, Kushner et al. have reported that transgenic PDX1 expression restored β cell mass and pancreatic function in *IRS2*$^{-/-}$ mice, a model that displays increased β cell apoptosis (54). These findings provide important support for the hypothesis that PDX1 acts primarily through cell survival pathways in vivo and can modulate prosurvival insulin/IGF signaling.

The results of the present study suggest that PDX1-regulated apoptosis is physiologically important in the lifelong maintenance of β cell mass. Given the disruption in β cell/α cell organization and the altered islet morphology of *Pdx1*$^{+/-}$ islets, it is likely that a significant loss of *functional* β cell mass precedes measurable changes in *morphological* β cell mass. This is not unexpected, since subtle changes in pancreas physiology can be readily measured with accuracy using the perfused pancreas, whereas histological parameters such as β cell mass are more difficult to determine. According to a previous study (9), *morphological* β cell mass in *Pdx1*$^{+/-}$ pancreata is reduced at 15 weeks by 37% (*Pdx1*$^{+/-}$, 1.76 ± 0.13 mg vs. *Pdx1*$^{+/+}$, 2.8 ± 0.44 mg), whereas Shih and colleagues found no decrease in β cell area at a similar age (55). In experimental models such as *Pdx1*$^{+/-}$ mice, functional β cell mass may be substantially lower than β cell mass estimated using classical morphometric criteria because apoptotic or poorly functioning islets are still counted if they contain insulin.

The specialized architecture and relative distribution of islet cell types may also play important roles in islet function and survival. For example, disruption of contacts between β cells may reduce the secretory efficiency of islets, thereby requiring higher (potentially toxic) levels of $Ca^{2+}$ to maintain secretion. We detected striking changes in islet architecture in *Pdx1*$^{+/-}$

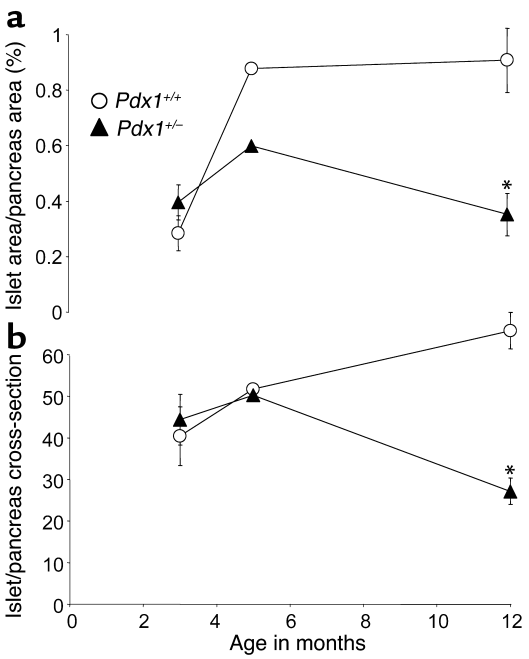


**Figure 10**
Reduced β cell mass and islet number in *Pdx1*$^{+/-}$ mice. (**a**) Islet cell area at 3, 5, and 12 months was estimated using insulin immunoreactivity as described in Methods and normalized to the total pancreatic cross-sectional area. Four sections were analyzed from each animal. (**b**) The number of islets was counted in complete pancreatic sections at low magnification (1.25× objective). Asterisks denote significant difference from wild type. Number of mice studied at 3 months, 5 months, and 12 months, respectively: *Pdx1*$^{+/+}$, *n* = 4, 2, and 5; *Pdx1*$^{+/-}$, *n* = 4, 2, and 4.

mice as an early defect. Similarly, islets with conditional deletion of PDX1 displayed a marked loss of the typical islet architecture (11). Whether this is a cause or effect of enhanced apoptosis remains to be determined. It has been suggested that specific binding of PDX1 to the glucagon promoter (14) may be important for the suppression of the default α cell developmental pathway of β cell precursors. Thus, it is possible that apoptosis caused by PDX1 deficiency leads to, or is associated with, relative dedifferentiation of some islets/β cells and the relative enhancement of a pool of less differentiated islet cells. In the β cell–specific PDX1 knockout model, approximately 22% of insulin-positive cells also expressed glucagon (11). Our study clearly shows that PDX1 is important not only in the normal development of the islet but also plays a critical role in the maintenance of normal islet function later in life by determining the balance of cellular proliferation and death (20).

A major finding of the present study is that a 50% reduction in PDX1 gene expression is still compatible with normal glucose sensing, insulin gene expression, or stimulus-secretion coupling in isolated islets and β cells. Although several lines of evidence have suggested a paramount role for PDX1 in pancreatic genesis and islet development, whether PDX1 plays specific physiological roles in fully differentiated β cells has remained less clear. For example, glucose has been shown to phosphorylate PDX1 and to activate PDX1 DNA binding activity (53, 56). Glucose-stimulated changes in the subcellular location of PDX1 have also been reported by certain groups (57). However, the exact relationship between these events and changes in the function of maximally differentiated β cells remain unclear.

The major physiological role ascribed to PDX1 in the adult β cell is the control of insulin gene expression (8). In support of this hypothesis, PDX1 transfection permitted the elevation of insulin mRNA in response to high glucose in the PDX1–deficient NES2Y cell line derived from a patient with persistent hyperinsulinemic hypoglycemia of infancy (58). Other evidence for the involvement of PDX1 in insulin expression comes from the ability of PDX1 to promote ectopic insulin expression in the presence of other transcription factors (16, 59). However, results from the present study and others (11, 13, 55) suggest a less important role for PDX1 in the regulation of insulin mRNA and protein levels in vivo. Clearly, pancreatic insulin content and gene expression are normal at a time when PDX1 levels are significantly reduced, but become abnormal only in older, more overtly diabetic mice. Even then, part of the reduction in pancreatic insulin content may be accounted for by a reduced number of islets. In other studies, while PDX1 cotransfection potentiated the ability of other factors to activate insulin expression in non–β cells, this transfection alone was not sufficient (60). Similarly, there are now many examples in the literature where no correlation between PDX1 and insulin expression is found, including PDX1-positive cells expanded from human islets (61), antisense-treated MIN6 cells (62), and an insulin-secreting tumor (63). Perhaps most importantly, PDX1 is expressed at some level in several other cell types of the pancreas and foregut, whereas insulin is not (64). Therefore, evidence that PDX1 is either necessary or sufficient to drive a significant proportion of β cell insulin expression in vivo has not yet been presented. Interestingly, *Psammomys obesus* islets and NES2Y cells express high basal levels of insulin despite PDX1 deficiency, but show marked defects in glucose-stimulated insulin gene expression (35, 65). Perhaps PDX1 is involved, directly or indirectly, in glucose-stimulated insulin gene transcription, but is redundant for the control of basal insulin levels under normal conditions in vivo. Studies of insulin levels in single PDX1-deficient β cells are required.

Our measurements of normal pancreatic insulin content, islet insulin staining, and islet insulin mRNA in young $Pdx1^{+/-}$ mice suggest that apoptosis and the insulin secretory defects seen in vivo precede any effects on insulin levels. It is therefore likely that the reduction of pancreatic insulin content that accompanies reduced β cell mass, islet number, and alterations in islet architecture is secondary to increased β cell apoptosis. Whereas insulin gene expression was reduced in apoptotic human islets cultured in high glucose (41), we did not find significant differences in insulin mRNA under acute apoptotic conditions in normal wild-type mouse islets, suggesting a requirement for chronic exposure.

Our in vivo data confirm the findings of several other groups using global $Pdx1^{+/-}$, β cell–specific $Pdx1^{-/-}$, and inducible transgenic PDX1 knockdown mice (9–13). Our measurements of insulin secretion in response to glucose in the perfused whole pancreas are similar to those recently reported for another strain of $Pdx1^{+/-}$ mice (13). However, building on these previous observations to include the characterization of glucose signaling and insulin secretion from isolated islets and single cells has led to a greater appreciation of the complexity of the $Pdx1^{+/-}$ phenotype. In addition, our study provides an example wherein the assumption that the response of the whole pancreas can be recapitulated in individual isolated islets may not always be correct. Likewise, the heterogeneous responses of single cells are more complex than would be predicted from the activity of whole islets. Unfortunately, many studies of transgenic mice, from which conclusions regarding the cell biology or biophysics of a certain cell type are made, fail to test such assumptions by examining single cells. Our study also makes clear how difficult it can be to dissociate physiology from development in such experiments.

In addition to the role of PDX1 in MODY4, recent studies of European families have suggested that mutations in the *PDX1* gene may predispose to type 2 diabetes (8). Interestingly, deficiency in HNF-1α (MODY2) selectively promotes $Bcl_{XL}$-sensitive apoptosis at physiological

glucose levels in INS-1 cells (66), implying the existence of a common pathway regulating apoptosis that may contribute to both MODY and type 2 diabetes. As in the *Psammomys obesus* model, continuous nutrient stress may be necessary to induce pathological consequences. Our data show that partial PDX1 deficiency has the greatest effect later in life. The age-dependent progression to type 2 diabetes makes $Pdx1^{+/-}$ mice one of the most realistic animal models of the disease where the pancreatic defect is the primary cause. Examination of middle-aged mice revealed that the function of PDX1 persists through adulthood, resulting in β cell mass and islet numbers roughly halfway between that of wild-type mice and $Pdx1^{-/-}$ mice (which have no islets). The process by which PDX1 heterozygosity is compensated for until after 3 months of age is unknown, but may represent an important target pathway for therapeutic intervention in type 2 diabetes. For example, it has recently been shown that reducing PDX1 in βTC3 cells activates the PDX1 promoter, suggesting that PDX1 levels are partially controlled in an autoregulatory loop (12). In summary, our data indicate that partial PDX1 deficiency leads to organ-level defects in insulin secretion by complex mechanisms that include islet apoptosis and disrupted islet architecture, but not a ubiquitous or cell-autonomous defect in β cell stimulus-secretion coupling. Hence, a more complete understanding of the roles of PDX1 and apoptosis in the maintenance of functional β cell mass may point to novel approaches to slow the progression of diabetes mellitus.

## Acknowledgments

This work was supported by NIH grants to K.S. Polonsky (DK-31842 and DK-44860), S. Misler (DK-37380), and the Diabetes Research and Training Center at Washington University School of Medicine (P60 DK-20579). The support of the Blum Kovler Foundation is also gratefully acknowledged. We thank Ernesto Bernal-Mizrachi and Matteo Levisetti for helpful comments, William Pugh for expert technical assistance with the perfused pancreas, and Eric Ford for technical assistance and islet isolation. The assistance of Seamus Sreenan, Yun-Ping Zhou, and Diane Ostrega is also acknowledged. J.D. Johnson was supported by fellowship awards from the Juvenile Diabetes Research Foundation and the Natural Science and Engineering Research Council of Canada.

1. Sommer, R.J., et al. 1998. The Pristionchus HOX gene Ppa-lin-39 inhibits programmed cell death to specify the vulva equivalence group and is not required during vulval induction. *Development.* **125**:3865–3873.
2. Rhinn, M., Dierich, A., Le Meur, M., and Ang, S. 1999. Cell autonomous and non-cell autonomous functions of Otx2 in patterning the rostral brain. *Development.* **126**:4295–4304.
3. Izon, D.J., et al. 1998. Loss of function of the homeobox gene Hoxa-9 perturbs early T-cell development and induces apoptosis in primitive thymocytes. *Blood.* **92**:383–393.
4. Dear, T.N., et al. 1995. The Hox11 gene is essential for cell survival during spleen development. *Development.* **121**:2909–2915.
5. Offield, M.F., et al. 1996. PDX-1 is required for pancreatic outgrowth and differentiation of the rostral duodenum. *Development.* **122**:983–995.
6. Jonsson, J., Carlsson, L., Edlund, T., and Edlund, H. 1994. Insulin-promoter-factor 1 is required for pancreas development in mice. *Nature.* **371**:606–609.
7. Stoffers, D.A., Zinkin, N.T., Stanojevic, V., Clarke, W.L., and Habener, J.F. 1997. Pancreatic agenesis attributable to a single nucleotide deletion in the human IPF1 gene coding sequence. *Nat. Genet.* **15**:106–110.
8. McKinnon, C.M., and Docherty, K. 2001. Pancreatic duodenal homeobox-1, PDX-1, a major regulator of beta cell identity and function. *Diabetologia.* **44**:1203–1214.
9. Dutta, S., Bonner-Weir, S., Montminy, M., and Wright, C. 1998. Regulatory factor linked to late-onset diabetes? *Nature.* **392**:560.
10. Lottmann, H., Vanselow, J., Hessabi, B., and Walther, R. 2001. The Tet-On system in transgenic mice: inhibition of the mouse pdx-1 gene activity by antisense RNA expression in pancreatic beta-cells. *J. Mol. Med.* **79**:321–328.
11. Ahlgren, U., Jonsson, J., Jonsson, L., Simu, K., and Edlund, H. 1998. beta-cell-specific inactivation of the mouse Ipf1/Pdx1 gene results in loss of the beta-cell phenotype and maturity onset diabetes. *Genes Dev.* **12**:1763–1768.
12. Thomas, M.K., et al. 2001. Development of diabetes mellitus in aging transgenic mice following suppression of pancreatic homeoprotein IDX-1. *J. Clin. Invest.* **108**:319–329. doi:10.1172/JCI200112029.
13. Brissova, M., et al. 2002. Reduction in pancreatic transcription factor PDX-1 impairs glucose-stimulated insulin secretion. *J. Biol. Chem.* **227**:11225–11232.
14. Chakrabarti, S.K., James, J.C., and Mirmira, R.G. 2002. Quantitative assessment of gene targeting in vitro and in vivo by the pancreatic transcription factor, Pdx1. Importance of chromatin structure in directing promoter binding. *J. Biol. Chem.* **277**:13286–13293.
15. Ohlsson, H., Karlsson, K., and Edlund, T. 1993. IPF1, a homeodomain-containing transactivator of the insulin gene. *EMBO J.* **12**:4251–4259.
16. Serup, P., et al. 1996. Induction of insulin and islet amyloid polypeptide production in pancreatic islet glucagonoma cells by insulin promoter factor 1. *Proc. Natl. Acad. Sci. U. S. A.* **93**:9015–9020.
17. Macfarlane, W.M., et al. 2000. Glucose regulates islet amyloid polypeptide gene transcription in a PDX1- and calcium-dependent manner. *J. Biol. Chem.* **275**:15330–15335.
18. Watada, H., et al. 1996. The human glucokinase gene beta-cell-type promoter: an essential role of insulin promoter factor 1/PDX-1 in its activation in HIT-T15 cells. *Diabetes.* **45**:1478–1488.
19. Waeber, G., Thompson, N., Nicod, P., and Bonny, C. 1996. Transcriptional activation of the GLUT2 gene by the IPF-1/STF-1/IDX-1 homeobox factor. *Mol. Endocrinol.* **10**:1327–1334.
20. Bonner-Weir, S. 2000. Perspective: postnatal pancreatic beta cell growth. *Endocrinology.* **141**:1926–1929.
21. Pontoglio, M., et al. 1998. Defective insulin secretion in hepatocyte nuclear factor 1α-deficient mice. *J. Clin. Invest.* **101**:2215–2222.
22. Lacy, P.E., and Kostianovsky, M. 1967. Method for the isolation of intact islets of Langerhans from the rat pancreas. *Diabetes.* **16**:35–39.
23. Zhou, Y.P., et al. 2000. Overexpression of Bcl-x(L) in beta-cells prevents cell death but impairs mitochondrial signal for insulin secretion. *Am. J. Physiol. Endocrinol. Metab.* **278**:E340–E351.
24. Grynkiewicz, G., Poenie, M., and Tsien, R.Y. 1985. A new generation of Ca2+ indicators with greatly improved fluorescence properties. *J. Biol. Chem.* **260**:3440–3450.
25. Johnson, J.D., Van Goor, F., Wong, C.J., Goldberg, J.I., and Chang, J.P. 1999. Two endogenous gonadotropin-releasing hormones generate dissimilar Ca(2+) signals in identified goldfish gonadotropes. *Gen. Comp. Endocrinol.* **116**:178–191.
26. Barnett, D.W., and Misler, S. 1997. An optimized approach to membrane capacitance estimation using dual-frequency excitation. *Biophys. J.* **72**:1641–1658.
27. Zhou, Y.P., et al. 1998. Apoptosis in insulin-secreting cells. Evidence for the role of intracellular Ca2+ stores and arachidonic acid metabolism. *J. Clin. Invest.* **101**:1623–1632.
28. Fadok, V.A., et al. 1992. Exposure of phosphatidylserine on the surface of apoptotic lymphocytes triggers specific recognition and removal by macrophages. *J. Immunol.* **148**:2207–2216.
29. Wong, H., Anderson, W.D., Cheng, T., and Riabowol, K.T. 1994. Monitoring mRNA expression by polymerase chain reaction: the "primer-dropping" method. *Anal. Biochem.* **223**:251–258.
30. Gillis, K.D., and Misler, S. 1993. Enhancers of cytosolic cAMP augment depolarization-induced exocytosis from pancreatic B-cells: evidence for effects distal to Ca2+ entry. *Pflugers Arch.* **424**:195–197.
31. Raman, V., et al. 2000. Compromised HOXA5 function can limit p53 expression in human breast tumours. *Nature.* **405**:974–978.
32. Quaggin, S.E., Yeger, H., and Igarashi, P. 1997. Antisense oligonucleotides to Cux-1, a Cut-related homeobox gene, cause increased apoptosis in mouse embryonic kidney cultures. *J. Clin. Invest.* **99**:718–724.
33. Shimamoto, T., Nakamura, S., Bollekens, J., Ruddle, F.H., and Takeshita, K. 1997. Inhibition of DLX-7 homeobox gene causes decreased expression of GATA-1 and c-myc genes and apoptosis. *Proc. Natl. Acad. Sci. U. S. A.* **94**:3245–3249.

34. Shimamoto, T., Ohyashiki, K., and Takeshita, K. 2000. Overexpression of the homeobox gene DLX-7 inhibits apoptosis by induced expression of intercellular adhesion molecule-1. *Exp. Hematol.* **28**:433–441.
35. Leibowitz, G., et al. 2001. IPF1/PDX1 deficiency and beta-cell dysfunction in Psammomys obesus, an animal with type 2 diabetes. *Diabetes.* **50**:1799–1806.
36. Leibowitz, G., et al. 2001. Beta-cell glucotoxicity in the Psammomys obesus model of type 2 diabetes. *Diabetes.* **50**:S113–S117.
37. Donath, M.Y., Gross, D.J., Cerasi, E., and Kaiser, N. 1999. Hyperglycemia-induced beta-cell apoptosis in pancreatic islets of Psammomys obesus during development of diabetes. *Diabetes.* **48**:738–744.
38. Seufert, J., Weir, G.C., and Habener, J.F. 1998. Differential expression of the insulin gene transcriptional repressor CCAAT/enhancer-binding protein β and transactivator islet duodenum homeobox-1 in rat pancreatic β cells during the development of diabetes mellitus. *J. Clin. Invest.* **101**:2528–2539.
39. Harmon, J.S., et al. 1999. In vivo prevention of hyperglycemia also prevents glucotoxic effects on PDX-1 and insulin gene expression. *Diabetes.* **48**:1995–2000.
40. Stoffers, D.A., et al. 2000. Insulinotropic glucagon-like peptide 1 agonists stimulate expression of homeodomain protein IDX-1 and increase islet size in mouse pancreas. *Diabetes.* **49**:741–748.
41. Marshak, S., et al. 1999. Impaired beta-cell functions induced by chronic exposure of cultured human pancreatic islets to high glucose. *Diabetes.* **48**:1230–1236.
42. Gremlich, S., Bonny, C., Waeber, G., and Thorens, B. 1997. Fatty acids decrease IDX-1 expression in rat pancreatic islets and reduce GLUT2, glucokinase, insulin, and somatostatin levels. *J. Biol. Chem.* **272**:30261–30269.
43. Cnop, M., Hannaert, J.C., Hoorens, A., Eizirik, D.L., and Pipeleers, D.G. 2001. Inverse relationship between cytotoxicity of free fatty acids in pancreatic islet cells and cellular triglyceride accumulation. *Diabetes.* **50**:1771–1777.
44. Olson, L.K., et al. 1995. Reduction of insulin gene transcription in Hit-T15 beta cells chronically exposed to a supraphysiological glucose concentration is associated with loss of STF-1 transcription factor expression. *Proc. Natl. Acad. Sci. U. S. A.* **92**:9127–9131.
45. Sharma, A., Olson, L.K., Robertson, R.P., and Stein, R. 1995. The reduction of insulin gene transcription in Hit-T15 beta cells chronically exposed to high glucose concentration is associated with the loss of RIPE3b1 and STF-1 transcription factor expression. *Mol. Endocrinol.* **9**:1127–1134.
46. Zangen, D.H., et al. 1997. Reduced insulin, GLUT2, and IDX-1 in beta-cells after partial pancreatectomy. *Diabetes.* **46**:258–264.
47. Stoffers, D.A., Ferrer, J., Clarke, W.L., and Habener, J.F. 1997. Early-onset type-II diabetes mellitus (MODY4) linked to IPF1. *Nat. Genet.* **17**:138–139.
48. Hani, E.H., et al. 1999. Defective mutations in the insulin promoter factor-1 (IPF-1) gene in late-onset type 2 diabetes mellitus. *J. Clin. Invest.* **104**:R41–R48.
49. Macfarlane, W.M., et al. 1999. Missense mutations in the insulin promoter factor-1 gene predispose to type 2 diabetes. *J. Clin. Invest.* **104**:R33–R39.
50. Johnson, J.D., and Chang, J.P. 2000. Function- and agonist-specific Ca2+ signalling: the requirement for and mechanism of spatial and temporal complexity in Ca2+ signals. *Biochem. Cell Biol.* **78**:217–240.
51. Berridge, M.J., Bootman, M.D., and Lipp, P. 1998. Calcium—a life and death signal. *Nature.* **395**:645–648.
52. Nakai, J., et al. 2002. Regulation of insulin action and pancreatic beta-cell function by mutated alleles of the gene encoding forkhead transcription factor Foxo1. *Nat. Genet.* **32**:245–253.
53. Wu, H., et al. 1999. Insulin stimulates pancreatic-duodenal homoeobox factor-1 (PDX1) DNA-binding activity and insulin promoter activity in pancreatic beta cells. *Biochem. J.* **344**:813–818.
54. Kushner, J.A., et al. 2002. Pdx1 restores β cell function in Irs2 knockout mice. *J. Clin. Invest.* **109**:1193–1201. doi:10.1172/JCI200214439.
55. Shih, D.Q., et al. 2002. Profound defects in pancreatic beta-cell function in mice with combined heterozygous mutations in Pdx-1, Hnf-1alpha, and Hnf-3beta. *Proc. Natl. Acad. Sci. U. S. A.* **99**:3818–3823.
56. Macfarlane, W.M., et al. 1999. Glucose stimulates translocation of the homeodomain transcription factor PDX1 from the cytoplasm to the nucleus in pancreatic beta-cells. *J. Biol. Chem.* **274**:1011–1016.
57. Elrick, L.J., and Docherty, K. 2001. Phosphorylation-dependent nucleocytoplasmic shuttling of pancreatic duodenal homeobox-1. *Diabetes.* **50**:2244–2252.
58. Macfarlane, W.M., et al. 2000. Glucose modulation of insulin mRNA levels is dependent on transcription factor PDX-1 and occurs independently of changes in intracellular Ca2+. *Diabetes.* **49**:418–423.
59. Ferber, S., et al. 2000. Pancreatic and duodenal homeobox gene 1 induces expression of insulin genes in liver and ameliorates streptozotocin-induced hyperglycemia. *Nat. Med.* **6**:568–572.
60. Glick, E., Leshkowitz, D., and Walker, M.D. 2000. Transcription factor BETA2 acts cooperatively with E2A and PDX1 to activate the insulin gene promoter. *J. Biol. Chem.* **275**:2199–2204.
61. Beattie, G.M., et al. 1999. Sustained proliferation of PDX-1(+) cells derived from human islets. *Diabetes.* **48**:1013–1019.
62. Kajimoto, Y., et al. 1997. Suppression of transcription factor PDX-1/IPF1/STF-1/IDX-1 causes no decrease in insulin mRNA in MIN6 cells. *J. Clin. Invest.* **100**:1840–1846.
63. Nakamura, T., et al. 2001. Insulin production in a neuroectodermal tumor that expresses islet factor-1, but not pancreatic-duodenal homeobox 1. *J. Clin. Endocrinol. Metab.* **86**:1795–1800.
64. Kawaguchi, Y., et al. 2002. The role of the transcriptional regulator Ptf1a in converting intestinal to pancreatic progenitors. *Nat. Genet.* **32**:128–134.
65. MacFarlane, W.M., et al. 1999. Engineering a glucose-responsive human insulin-secreting cell line from islets of Langerhans isolated from a patient with persistent hyperinsulinemic hypoglycemia of infancy. *J. Biol. Chem.* **274**:34059–34066.
66. Wobser, H., et al. 2002. Dominant-negative suppression of HNF-1 alpha results in mitochondrial dysfunction, INS-1 cell apoptosis, and increased sensitivity to ceramide-, but not to high glucose-induced cell death. *J. Biol. Chem.* **277**:6413–6421.